Chinese Journal of Physiology 54(1): 19-29, 2011
DOI: 10.4077/CJP.2011.AMM002

Contribution of Non-Inactivating Na^+ Current Induced by Oxidizing Agents to the Firing Behavior of Neuronal Action Potentials: Experimental and Theoretical Studies from NG108-15 Neuronal Cells

Sheng-Nan Wu[1, 2], Yi-Ching Lo[3], Ai-Yu Shen[4], and Bing-Shuo Chen[2, 5]

[1]*Department of Physiology, National Cheng Kung University Medical College, Tainan*
[2]*Institute of Basic Medical Sciences, National Cheng Kung University Medical College, Tainan*
[3]*Department of Pharmacology, Kaohsiung Medical University, Kaohsiung*
[4]*Institute of Medical and Health Sciences, Fooyin University, Kaohsiung*
and
[5]*Department of Anesthesiology, Buddhist Tzu Chi General Hospital, Chiayi*
Taiwan, Republic of China

Abstract

The effects of chemical injury with oxidizing agents on voltage-gated Na^+ current (I_{Na}) in differentiated NG108-15 neuronal cells were investigated in this study. In whole-cell patch-clamp recordings, the challenge of these cells with *t*-butyl hydroperoxide (*t*-BHP; 1 mM) decreased the peak amplitude of I_{Na} with no modification in the current-voltage relationship. It caused a slowing of current inactivation, although there was no alteration in the activation time course of I_{Na}. Cell exposure to *t*-BHP also increased a non-inactivating I_{Na} ($I_{Na(NI)}$) elicited by long-lasting ramp pulses. The *t*-BHP-induced increase of $I_{Na(NI)}$ was reversed by a further application of riluzole (10 μM) or oxcarbazepine (10 μM). When I_{Na} was elicited by simulated waveforms of action potentials (APs), during exposure to *t*-BHP, the amplitude of this inward current was diminished, accompanied by a reduction in inactivation/deactivation rate and an increase in current fluctuations. Under current-clamp recordings, addition of *t*-BHP (0.3 mM) enhanced AP firing in combination with clustering-like activity and sub-threshold membrane oscillations. In the simulation study, when the fraction of non-inactivating Na_V channels was elevated, the simulated window component of I_{Na} in response to a long-lasting ramp pulse was reduced; however, the persistent I_{Na} was markedly enhanced. Moreover, when simulated firing of APs was generated from a modeled neuron, changes of AP firing caused by the increased fraction of non-inactivating Na_V channels used to mimic the *t*-BHP actions were similar to the experimental observations. Taken together, it is anticipated that the effects of oxidizing agents on $I_{Na(NI)}$ could be an important mechanism underlying their neurotoxic actions in neurons or neuroendocrine cells occurring *in vivo*.

Key Words: ***t*-butyl hydroperoxide, Na^+ current, non-inactivating Na^+ current, action potential, computer simulations**

Introduction

Voltage-gated Na^+ current (I_{Na}) is recognized to mediate the upstroke of the neuronal action potential (AP), and following an instantaneous activation, the current rapidly inactivates over time. However, imme-

Corresponding author: Dr. Sheng-Nan Wu, Department of Physiology, National Cheng Kung University, Medical College, No. 1, University Road, Tainan 70101, Taiwan, Republic of China. Tel: +886-6-2353535-5334, Fax: +886-6-2362780, E-mail: snwu@mail.ncku.edu.tw
http://phys.med.ncku.edu.tw/english/fac-snwu.php.
Received: January 11, 2010; Revised: March 4, 2010; Accepted: March 6, 2010.
 ISSN : 0304-4920. http://www.cps.org.tw

diately after the initial rapid inactivation, a certain fraction of non-inactivating I_{Na} ($I_{Na(NI)}$), caused by bursts and/or late scattered openings of single channels, actually remains active (14, 30). The $I_{Na(NI)}$, which is resistant to inactivation even during depolarizations lasting many seconds, has been demonstrated in a variety of neuronal types (8, 17, 31, 33, 35). Because this current shows either no or very slow inactivation, it may not directly be involved in production of the transient APs. However, it is thought to be associated with the control of membrane excitability in the voltage region just around the level of the sub-threshold required for spike generation (11, 33, 35). Such sub-threshold I_{Na} may, in turn, drive spontaneous spike discharges. This current can also produce a significant increase in intracellular Na^+ if it turns on for many seconds, thereby producing a state of Na^+ overload inside the cell (10, 21).

$I_{Na(NI)}$ has been demonstrated to be responsible for the fibrillations commonly seen in denervated skeletal muscle (12, 14, 24). Several heritable forms of myotonia and periodic paralysis are caused by impaired inactivation of Na^+ (Na_V) channels causing a non-inactivating component of I_{Na} ($I_{Na(P)}$) that may either initiate abnormal bursts of APs or cause paralysis by depolarizing fibers to a refractory, inexcitable state (3, 12, 24). Notably, oxcarbazepine is an anti-epileptogenic drug, whereas riluzole, a benzothiazole derivative, is a neuroprotective drug useful to treat amyotrophic lateral sclerosis, and both compounds were recently reported to inhibit the $I_{Na(NI)}$ more strongly than the rapidly activating I_{Na} (15, 33).

The high lipid content and oxygen metabolism of the brain are recognized to render it vulnerable to oxidative damage. This may be a result of increased levels of free radicals or compromised defenses (*e.g.*, antioxidant levels) against the production of oxygen radicals in the brain during oxidative stress (13, 25). Numerous reports have demonstrated the ability of oxidizing agents to modify the activity of ion channels (5, 16, 27, 29). However, how the oxidizing agents can affect the gating and amplitude of I_{Na} or $I_{Na(NI)}$ in neurons or neuroendocrine cells remains largely unknown.

The NG108-15 cell, which is a motor neuron-like cell line, has attracted growing interest as a suitable model for investigating the mechanisms of neuronal development and differentiation (18, 19, 22, 23). It is ideal for whole-cell biosensor applications, because of the inability to form synaptic connections and network activity in culture (22). In addition, the tetrodotoxin (TTX)-sensitive I_{Na}, which was identified in differentiated NG108-15 neuronal cells, appears to be primarily generated by the NaV1.7 channel which is encoded by the SCN9A gene (18). When NG108-15 cells were challenged with hydrogen peroxide, cell damage was associated with the decreased glutathione levels (28).

Accordingly, the goals of this study were to use an experimental and simulation approach for evaluation of the role of $I_{Na(NI)}$ in the electrophysiological behavior of NG108-15 neuronal cells and in investigations of the effects of oxidizing agents (*e.g.*, *t*-butyl hydroperoxide; *t*-BHP) on I_{Na} and $I_{Na(NI)}$ in these cells. Numerical simulations of $I_{Na(NI)}$ were found to reproduce the experimental results and showed that *t*-BHP-induced changes in AP firing tended to arise from the increased fraction of non-inactivating Na_V channels, while changes in the maximal conductance of I_{Na} or $I_{Na(NI)}$ remained unaltered. Therefore, the observations made in this study reveal that the fraction of non-inactivating Na_V channels can be altered by oxidizing agents and may play a pivotal role in inducing sub-threshold membrane oscillation with a clustering-like activity of AP firing.

Materials and Methods

Cell Preparations

The mouse neuroblastoma × rat glioma hybrid cell line (NG108-15) was originally obtained from the European Collection of Cell Cultures (ECACC-88112302; Wiltshire, UK). Cells were grown in monolayer cultures at a density of 10^6/ml in plastic disks containing Dulbecco's modified Eagle's medium supplemented with 100 μM hypoxanthine, 1 μM aminopterin, 16 μM thymidine, and 5% fetal bovine serum, in a humidified environment of 5% CO_2/95% air at 37°C. To induce neuronal differentiation, the culture medium was replaced with a medium containing 1 mM dibutyryl cyclic-AMP, and the cells were then maintained in an incubator for another 1-7 days (4, 19, 23). To observe neurite growth, a Nikon Eclipse Ti-E inverted microscope (Li Trading Co., Taipei, Taiwan, ROC) equipped with a five-megapixel cooled digital camera was used. The digital camera was connected to a personal computer controlled by NIS-Elements BR3.0 software (Nikon, Kanagawa, Japan). The number of neurites and varicosities was increased when cells were pre-incubated with 1 mM dibutyryl cyclic-AMP. Cell viability was evaluated using a WST-1 assay (Roche-Diagnostics, Indianapolis, IN, USA) and an ELISA reader (Dynatech, Chantilly, VA, USA).

Electrophysiological Measurements

Before electrophysiological experiments were made, cells were dissociated with 1% trypsin/EDTA solution, and an aliquot of cell suspension was transferred to a recording chamber affixed to the stage of

a DM-IL inverted microscope (Leica, Wetzlar, Germany). Cells were bathed at room temperature (20-25°C) in normal Tyrode's solution containing 1.8 mM $CaCl_2$. The electrodes were pulled from Kmax-51 capillaries (Kimble Glass, Vineland, NJ, USA) in a PP-830 puller (Narishige, Tokyo, Japan), which had a resistance of 3-5 MΩ when filled with different intracellular solutions, and were subsequently mounted on and controlled by a WR-98 hydraulic micromanipulator (Narishige, Tokyo, Japan). Patch-clamp recordings were carried out in whole-cell configuration using an RK-400 amplifier (Bio-Logic, Claix, France) or an Axopatch-200B amplifier (Molecular Devices, Sunnyvale, CA, USA). Tested compounds were applied by perfusion or added to the bath to obtain the final concentration indicated.

Data Recordings and Analyses

The signals were displayed on an HM-507 oscilloscope (Hameg, East Meadow, NY, USA) and a liquid crystal projector (AV600; Delta, Taipei, Taiwan, ROC). The data were stored online in a TravelMate-6253 laptop computer (Acer, Taipei, Taiwan, ROC) at 10 kHz through a Digidata-1322A interface (Molecular Devices). The latter device was equipped with an Adaptec SlimSCSI card (Milpitas, CA, USA) *via* a PCMCIA slot, and controlled by pCLAMP 9.2 (Molecular Devices). Current signals were low-pass filtered at 1 or 3 KHz. The signals were analyzed using pCLAMP 9.2 (Molecular Devices), Origin 7.5 (OriginLab, Northampton, MA, USA), SigmaPlot 7.0 (SPSS Inc., Apex, NC, USA), or custom-made macros in Excel 2007 spreadsheet running under Windows Vista (Microsoft, Redmond, WA, USA). The pCLAMP-generated voltage-step protocols were used to evaluate the current-voltage (*I-V*) relationships for ion currents (*e.g.*, I_{Na}). In another set of experiments, the simulated waveforms of APs from a modeled neuron used as voltage templates were replayed to NG108-15 cells through a digital-analog converter to evoke I_{Na} (Digidata 1322A) (4, 15, 20).

To evaluate the $I_{Na(NI)}$ in NG108-15 neuronal cells, the ramp voltage-clamp pulses from -100 to +40 mV with different durations were applied to the cell at a frequency of 0.05 Hz. The amplitude of total $I_{Na(NI)}$ elicited by ramp pulse was measured as the maximal inward deflection of current. The current trajectory of I_{Na} inactivation obtained with or without application of oxidizing agents (*e.g.*, *t*-BHP) was fitted by a two-exponential process with the use of Origin 7.5 (OriginLab).

Values are provided as means ± standard error of the mean (S.E.M.). Values of 'n' indicate the number of cells from which the data were obtained. The paired or unpaired Student's *t* test and one-way analysis of variance with a least-significance difference method for multiple comparisons were used for the statistical evaluation of difference among means. Statistical analyses were performed using SPSS 14.0 (SPSS Inc., Chicago, IL, USA). The level of statistical significance was set at $P < 0.05$.

Drugs and Solutions

2,2'-Azo-bis(2-aminopropane) dihydrochloride (AAPH) was obtained from Wako Pure Industries (Osaka, Japan), riluzole (Rilutek®) was from Tocris Cookson, Ltd. (Bristol, UK), and oxcarbazepine (Tripetal®) was from Novartis Pharma AG (Basle, Switzerland). *t*-Butyl hydroperoxide (*t*-BHP), dibutyryl cyclic-AMP, tetraethylammonium chloride (TEA) and tetrodotoxin (TTX) were purchased from Sigma (St. Louis, MO, USA). Tissue culture media and trypsin/EDTA were obtained from Invitrogen (Carlsbad, CA, USA). All other chemicals, including $CsCl_2$, CsOH and $CdCl_2$, were of laboratory grade obtained from standard sources. The twice-distilled water that had been deionized through a Milipore-Q system (Millipore, Bedford, MA, USA) was used in all experiments.

The composition of a standard Hepes-buffered normal Tyrode's solution was as follows (in mM): NaCl 136.5, KCl 5.4, $CaCl_2$ 1.8, $MgCl_2$ 0.53, glucose 5.5, and Hepes-NaOH buffer 5.5 (pH 7.4). To record membrane potential, the patch pipette was filled with a solution (in mM): KCl 140, $MgCl_2$ 1, Na_2ATP 3, Na_2GTP 0.1, EGTA 0.1, and Hepes-KOH buffer 5 (pH 7.2). To measure I_{Na} or $I_{Na(NI)}$, K^+ ions inside the pipette solution were replaced with equimolar Cs^+ ions, and the pH was adjusted to 7.2 with CsOH.

Computer Simulations

To mimic the biophysical properties of spontaneous APs in differentiated NG108-15 neuronal cells, a cell model described previously (34) was modified and implemented. The basic model consists of an I_{Na} current, a delayed rectifier K^+ current (I_{Kdr}), and an *erg* (*ether-à-go-go*-related-gene) K^+ current (I_{erg}) (34).

For total I_{Na}, the modified Hodgkin-Huxley scheme plus a non-inactivating current was used according to the following equation:

$$I_{Na} = (1 - f) \times G_{Naf} \times m^3 \times h \times (V - V_{Na}) + f \times G_{NaNI} \times m \times (V - V_{Na}),$$

where G_{Naf} is the maximal conductance of rapidly activating I_{Na}, G_{NaNI} is the maximal conductance of $I_{Na(NI)}$, V is the membrane potential, V_{Na} is the Na^+ reversal potential, and m and h are voltage-dependent activation and inactivation variables, respectively. The f represents the fraction of the non-inactivating

Table 1. Default parameter values used for the modeling of NG108-15 neuronal cells differentiated with dibutyryl cyclic-AMP

Symbol	Description	Value
C_m	Membrane capacitance (μF)	1
G_{Naf}	Rapidly activating Na^+ current conductance (mS cm^{-2})	18
G_{NaNI}	Non-inactivating Na^+ current conductance (mS cm^{-2})	0.15
G_{Kdr}	Delayed rectifier K^+ current conductance (mS cm^{-2})	8.1
$G_{K(erg)}$	*erg*-like K^+ current conductance[a] (mS cm^{-2})	4.2
G_L	Leak current conductance (mS cm^{-2})	0.03
V_{Na}	Na^+ reversal potential (mV)	50
V_K	K^+ reversal potential (mV)	-80
V_L	Reversal potential for leak current (mV)	-54

[a]*erg: ether-à-go-go*-related gene.

Na_V channels.

The rate constants for I_{Na} used in the simulation here are described by the following equations:

$$\alpha_m = \frac{0.1(V + 40)}{\{1 - \exp[-0.09(V + 40)]\}},$$

$$\beta_m = 4\exp[-0.055(V + 70)],$$

$$\alpha_h = 0.07\exp[-0.05(V + 70)],$$

$$\beta_h = \frac{1}{\{1 - \exp[-0.09(V + 25)]\}}.$$

The single-compartment neuron model presented herein behaves according to the modified Hodgkin-Huxley scheme. Changes of membrane potential in this model (34) are described by the following membrane equation:

$$C_m\frac{dV}{dt} = -I_{Naf} - I_{Na(NI)} - I_{Kdr} - I_{erg} - g_L \times (V - V_L),$$

where C_m is the membrane capacitance and V is the membrane potential. The model equations used to generate these types of ion currents were previously described (34).

Simulations were undertaken using an Euler algorithm as implemented with the differential equation solver XPPaut on a Hewlett Packard (HP-xw9300) Workstation (Palo Alto, CA, USA) (9, 34). The source file for the model used in this study is available at http://senselab.med.yale.edu/modeldb. Parts of simulations were validated in Microsoft Excel (32). In the present simulations, the conductance values and reversal potentials, together with other default parameters, used to solve the set of differential equations are listed in Table 1.

Results

Effect of I_{Na} by t-BHP in Differentiated NG108-15 Neuronal Cells

In an initial set of electrophysiological experiments, we investigated the possible effects of *t*-BHP on I_{Na} elicited by step depolarizations in these cells. The experiments were conducted with a Cs^+-containing pipette solution and cells were bathed in Ca^{2+}-free Tyrode's solution containing 0.5 mM $CdCl_2$ and 10 mM TEA. As shown in Fig. 1, the cell was depolarized from -80 to -10 mV with a duration of 50 ms, and the rapidly activating I_{Na} could be elicited. When cells were challenged with *t*-BHP, the peak amplitude of I_{Na} was significantly diminished. For example, when cells were depolarized from -80 to -10 mV, addition of 1 mM *t*-BHP decreased the peak amplitude of I_{Na} from 1.13 ± 0.08 nA to 0.75 ± 0.07 nA (n = 7). After washout of *t*-BHP, the amplitude of I_{Na} was partially returned to 0.98 ± 0.08 nA (n = 5). Aside from the reduction of peak I_{Na}, a progressive slowing in the rate of current inactivation was clearly observed in the presence of *t*-BHP (Fig. 1B). For example, when cells were depolarized from -80 to -10 mV, during cell exposure to *t*-BHP (1 mM), the slow component of inactivation time constants for I_{Na} ($\tau_{inact(s)}$) *t*-BHP (1 mM) was significantly increased to 23.3 ± 1.6 ms from a control level of 17.6 ± 1.4 ms (n = 6). However, neither the activation time course of I_{Na} nor the fast component of current inactivation ($\tau_{inact(f)}$) could be modified in the presence of 1 mM *t*-BHP. Similarly, 2,2'-azo-bis(2-aminopropane) dihydrochloride (AAPH; 10 μM), known to be an azo compound that can general free radicals (16), could decrease the peak amplitude of I_{Na} accompanied by a significant reduction of current inactivation in NG108-15 neuronal cells (data not shown).

The effect of *t*-BHP on I_{Na} was next examined at the different levels of membrane potentials. In these experiments, each cell was held at -80 mV and different depolarizing pulses (50 ms in duration) were applied at a rate of 0.2 Hz. The *I-V* relationships of I_{Na} with and without application of 1 mM *t*-BHP were then constructed and plotted (Fig. 1C). The results showed

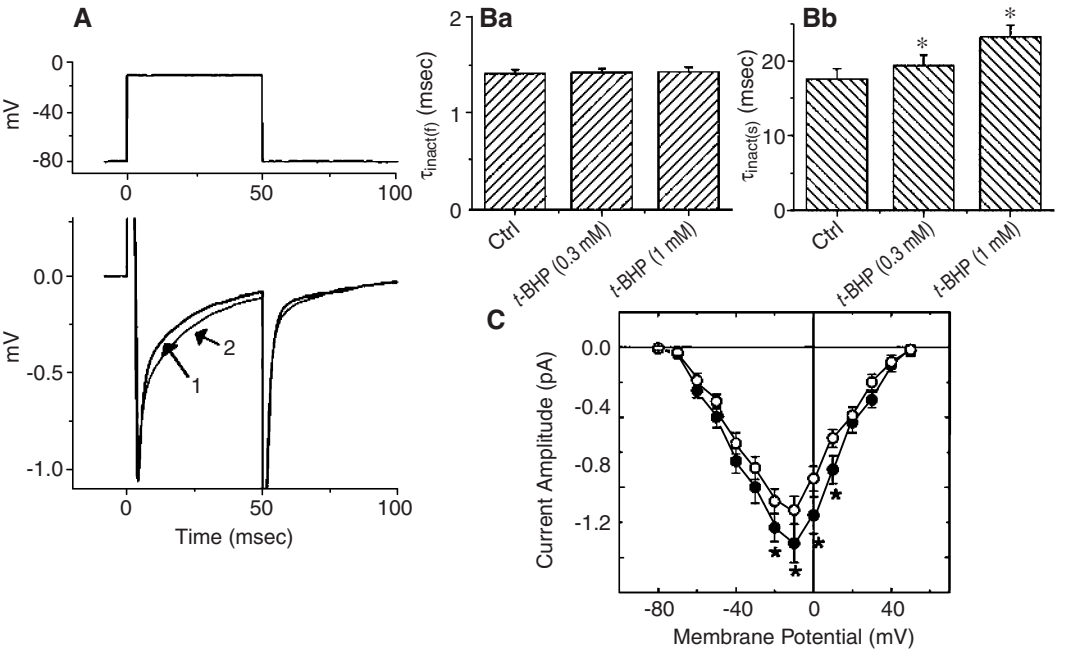

Fig. 1. Effect of *t*-BHP on I_{Na} in NG108-15 cells differentiated with 1 mM dibutyryl cAMP. In these experiments, cells were bathed in Ca^{2+}-free Tyrode's solution containing 0.5 mM $CdCl_2$ and 10 mM TEA. The pipette was filled with a Cs^+-containing solution. (A) Superimposed current traces obtained in the absence (*trace* 1, black) and presence (*trace* 2, gray) of 1 mM *t*-BHP. The upper part indicates the voltage protocol used. (B) Summary of data showing the effect of *t*-BHP on the time course for the fast ($\tau_{inact(f)}$) and slow ($\tau_{inact(s)}$) component of I_{Na} inactivation. Ctrl: control. Each bar represents means ± S.E.M. of data from 5-9 cells. *Significantly different from controls ($P < 0.05$). (C) Average *I-V* relationships of the peak I_{Na} obtained in control (●) and during exposure to 1 mM *t*-BHP (○). Each point shown in (C) represents the means ± S.E.M. (n = 6-11). Note that the overall *I-V* relationship of this current was not altered in the presence of *t*-BHP. *Significantly different from controls ($P < 0.05$).

that when 1 mM *t*-BHP was applied to the cells, the *I-V* relationship of I_{Na} was noted to remain unaltered, although there was a significant reduction in the peak amplitude of I_{Na}.

Stimulatory Effect of t-BHP on $I_{Na(NI)}$ in Differentiated NG108-15 Cells

$I_{Na(NI)}$, which can be responsible for initiation of neuronal APs, has been reported to be present in NG108-15 cells (15, 33). This current can activate within a few milliseconds upon depolarization, but either does not inactivate at all or only very slowly, thereby providing a steady inward current. Therefore, an additional series of whole-cell experiments were undertaken to evaluate whether oxidative injury with *t*-BHP has any effects on the amplitude of $I_{Na(NI)}$. In this set of experiments, cells were bathed in Ca^{2+}-free Tyrode's solution containing 0.5 mM $CdCl_2$ and 10 mM TEA. When the cell was held at the level of -60 mV, a long-lasting ramp pulse from -100 to +40 mV was then applied at a rate of 0.05 Hz. The rapid component of I_{Na} can be eliminated under these experimental conditions. The experimental results showed that unlike the transient component of I_{Na}, a progressive increase in the amplitude of $I_{Na(NI)}$ was observed during cell exposure to *t*-BHP (1 mM) (Fig. 2). For example, at a ramp of 0.07 V/s, the challenge of the cells with 1 mM *t*-BHP significantly increased the peak amplitude of $I_{Na(NI)}$ from 85 ± 12 to 132 ± 27 pA (n = 8). In addition, a subsequent application of riluzole (10 μM) or oxcarbazepine (10 μM) was able to reverse the increased amplitude of $I_{Na(NI)}$ in response to long-lasting ramp pulse. Riluzole (10 μM) and oxcarbazepine (10 μM) significantly diminished the peak amplitude of $I_{Na(NI)}$ by 43 ± 8% (n = 5) and 37 ± 6% (n = 6), respectively.

Effects of t-BHP on I_{Na} in Response to Simulated AP Waveforms

The size and time-course of ion currents (*e.g.*, I_{Na}) in response to changes in AP waveforms are different from those elicited by rectangular voltage-clamp pulses (4, 20). Therefore, the effects of *t*-BHP on I_{Na} elicited by the waveforms of APs generated from a modeled neuron were further investigated. In these experiments, the simulated waveforms of APs were generated as voltage templates and repeatedly replayed to evoke I_{Na} (15, 20). As shown in Fig. 3, the peak amplitude of I_{Na} in response to AP waveforms was diminished in the presence of 1 mM *t*-BHP. The

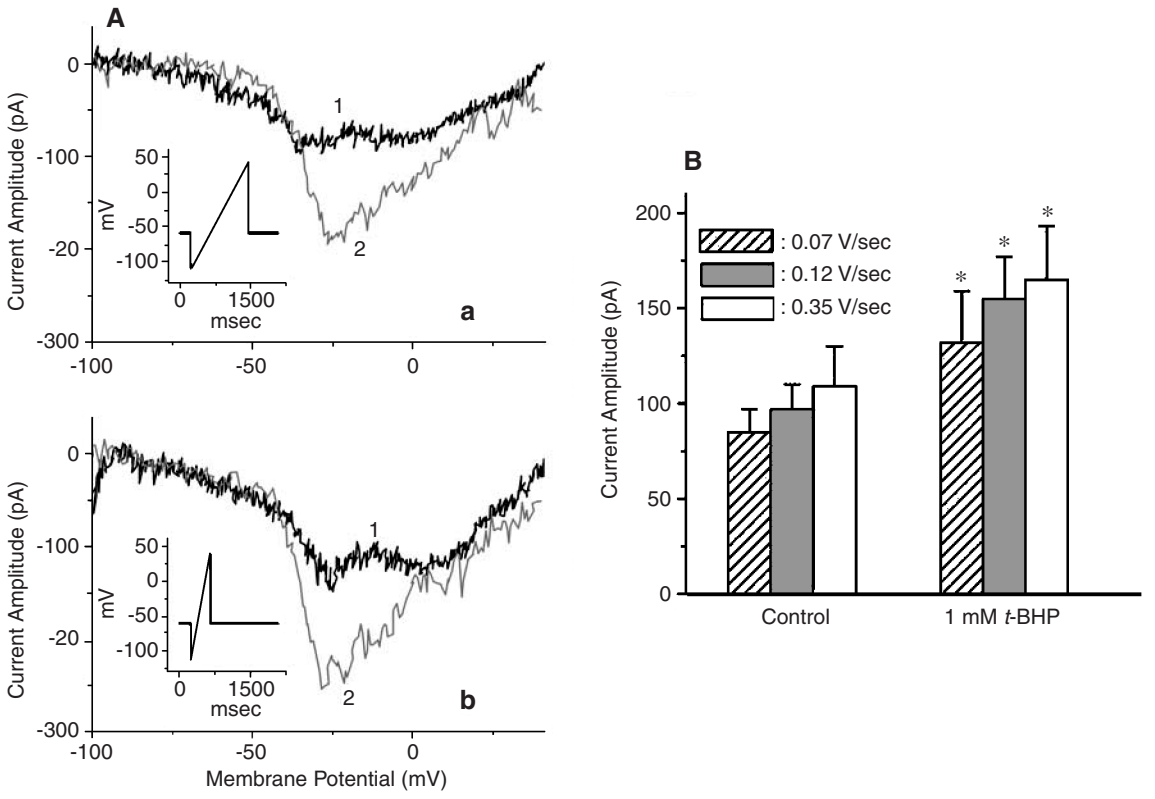

Fig. 2. Stimulatory effect of *t*-BHP on the $I_{Na(NI)}$ in differentiated NG108-15 cells. In these experiments, each cell was held at -60 mV and a long-lasting ramp pulse from -100 to +40 mV was applied. (A) Superimposed current traces elicited by ramp pulse from -100 to +40 mV with a duration of 1,200 ms (a) and 400 ms (b). *trace* 1 (black): control; *trace* 2 (gray): in the presence of 1 mM *t*-BHP. Insets shown in each panel of (A) indicate the voltage protocol used. (B) Summary of data showing the effect of *t*-BHP on the amplitude of $I_{Na(NI)}$ in different ramp rates (*i.e.*, 0.07, 0.12 and 0.35 V/s). Each bar represents means ± S.E.M. of data from 4-8 cells. *Significantly different from controls ($P < 0.05$).

challenge of the cells with *t*-BHP (1 mM) was also found to slow the inactivation/deactivation time course of I_{Na} in response to AP waveforms. It can be noted, interestingly, that current fluctuations at the level of holding potential emerge in the presence of *t*-BHP (Fig. 3B). In other words, when *t*-BHP was applied to the cell, the membrane exhibited large current fluctuations, along with the decreased amplitude of I_{Na} and the slowing of current inactivation/deactivation. Similar results were obtained in eight different cells examined.

Effect of t-BHP on the Firing of APs in Differentiated NG108-15 Cells

We next examined the possible effects of *t*-BHP on repetitive firing of APs. In these experiments, cells were bathed in normal Tyrode's solution containing 1.8 mM $CaCl_2$. Current-clamp recordings were made with a K^+-containing pipette solution. When the cells were challenged with *t*-BHP (0.3 mM), a progressive increase in the repetitive firing of APs was observed. Moreover, the firing patterns of cells were altered in the presence of *t*-BHP. There was a clustering activity in the firing pattern of APs in combination with the increased sub-threshold membrane oscillation (Fig. 4). That is, after clustering activity is terminated, a small, slow inward current is noted to develop over tens of milliseconds the course, which is associated with a parallel increase in the amplitude of sub-threshold oscillations. When NG108-15 cells were exposed to 1 mM *t*-BHP, the firing frequency of APs was significantly increased to 7.20 ± 0.04 Hz from a control value of 3.10 ± 0.03 Hz (n = 8).

Simulation Used to Mimic the Effect of t-BHP on $I_{Na(NI)}$ from the Modeled Neuron

To further elucidate the ionic mechanism of *t*-BHP actions in these cells, the simulated $I_{Na(NI)}$ was implemented. The detailed equation for this simulation was described in Materials and Methods. As shown in Fig. 5, the effect of *t*-BHP on simulated $I_{Na(NI)}$ in response to a long-lasting ramp pulse from -100 to +40 mV was found to closely resemble the experi-

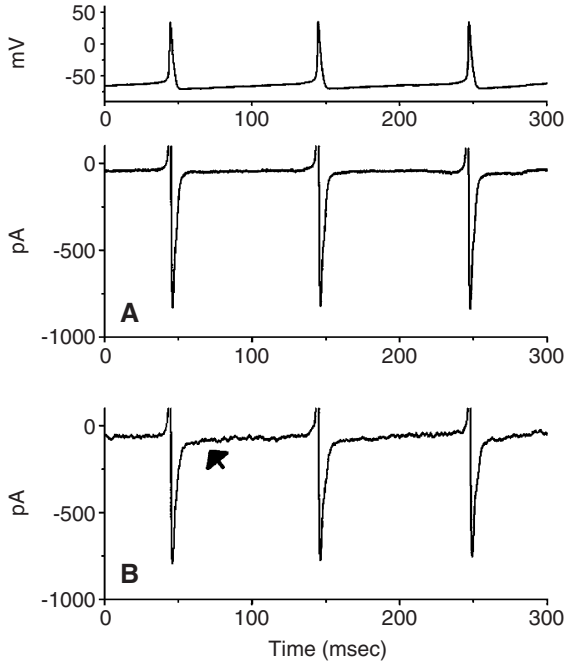

Fig. 3. Effect of *t*-BHP on AP waveform-evoked I_{Na} in differentiated NG108-15 cells. Current traces obtained in the absence (A) and presence of 1 mM *t*-BHP (B). The uppermost part shows the waveforms of APs which were generated from modeled neuron described in Materials and Methods. Notably, the time course of current inactivation/deactivation was modified during cell exposure to *t*-BHP. The arrow shown in (B) indicates the appearance of increased current fluctuations.

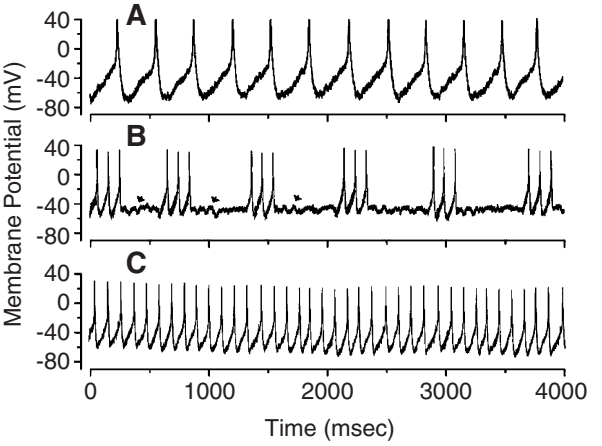

Fig. 4. Effect of *t*-BHP on the firing of APs in differentiated NG108-15 neuronal cells. The cells were bathed in normal Tyrode's solution containing 1.8 mM $CaCl_2$. Current-clamp recordings were made in these experiments. The patch pipettes were filled with a K^+-containing solution. Panel (A) is the control, and panel (B) and (C) were, respectively, recorded 2 min after the addition of 0.3 and 1 mM *t*-BHP. Notably, when cells were exposed to 0.3 mM *t*-BHP, clusters of APs interrupted by periods of sub-threshold membrane oscillations indicated by arrows in (B) were observed.

mental data shown in Fig. 2. The results show that the effect of *t*-BHP at a concentration of 1 mM can be mimicked by the increase of *f* value (*i.e.*, the fraction of $I_{Na(NI)}$) from 0.15 to 0.6. The window component of $I_{Na(NI)}$ ($I_{Na(W)}$) was decreased by 55% in the presence of 1 mM *t*-BHP, while the persistent component of $I_{Na(NI)}$ ($I_{Na(P)}$) was increased by around 4 folds. As a result, the total $I_{Na(NI)}$ generated by this model was found to be increased by around 2 fold. The simulation results are consistent with the experimental data showing that during the exposure to *t*-BHP (1 mM), current amplitude of $I_{Na(NI)}$ in response to long-lasting ramp pulse was increased, along with a decrease in the peak amplitude of I_{Na} and a slowing in current inactivation. These simulations clearly predict that exposure to *t*-BHP is capable of elevating the fraction of non-inactivating Na_V channels expressed in neurons or neuroendocrine cells. It is thus anticipated that oxidizing agents do not simply produce a reduction of the rapidly activating I_{Na}; however, they are also able to increase the amplitude of $I_{Na(P)}$.

Effect of t-BHP on Spontaneous APs in Modeled Neuron

Finally, in order to explore how oxidative injury with *t*-BHP can modify the firing pattern of APs in differentiated NG108-15 cells, a cell model was implemented to mimic the firing of neuronal APs. Spontaneous APs in these cells were mathematically reconstructed with the modeling of neuronal APs as described in Materials and Methods (34). As shown in Fig. 6, under control conditions, spontaneous APs were computationally generated at a rate of 3.3 Hz. When the fraction of non-inactivating Na_V channels (*i.e.*, *f* value) was arbitrarily reset to 0.4 from a control of 0.15, the pattern of spike discharge was greatly altered. Along with the increased firing of APs, clustering activity in combination with sub-threshold membrane oscillations can be identified. When the *f* value was further elevated to 0.6, bursting activity of APs no longer occurred; however, repetitive firing of simulated APs was greatly enhanced with a rate of 21.7 Hz. Based on this theoretical model, the results are similar to our experimental observations, which showed that the challenge of cells with *t*-BHP was able to alter the electrical behavior of NG108-15 cells. However, changes in the conductance values for I_{Na} or $I_{Na(NI)}$ do not appear to be required in order to mimic the effects of *t*-BHP on the firing pattern of simulated APs. Taken together, it is tempting to propose that the fraction of non-inactivating Na_V channels alone is sufficient to explain that, during the challenge of cells with oxidizing agents (*e.g.*, *t*-BHP), the firing pattern of neuronal APs, together with changes in I_{Na} and $I_{Na(NI)}$, can be altered in neurons

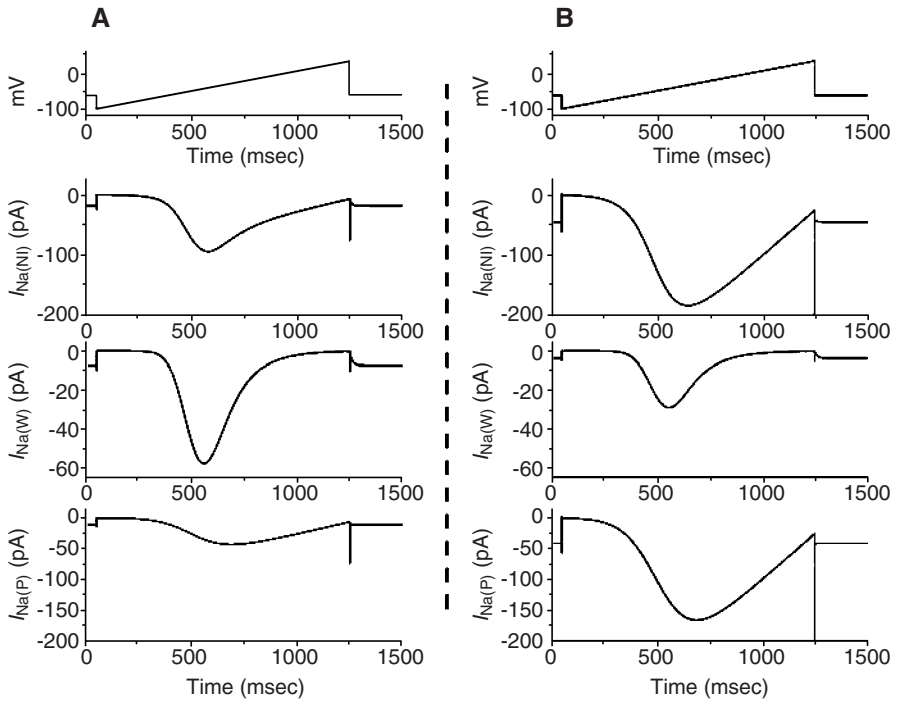

Fig. 5. Simulations of *t*-BHP effects on $I_{Na(NI)}$ elicited by a long-lasting ramp pulse in modeled neuron. The solutions to the ordinary differential equations were implemented in XPPaut software package. The values of G_{Naf} and G_{NaNI} were set at 49 and 4.5 mS/cm^2, respectively. The left (A) and right (B) sides, respectively, show simulated current traces which closely resemble the observed $I_{Na(NI)}$ obtained in the absence and presence of 1 mM *t*-BHP (Fig. 2). When the values of *f* was arbitrarily changed from 0.15 to 0.6, there was a reduction in current amplitude of $I_{Na(W)}$ in combination with the increased amplitude of $I_{Na(P)}$. The upper part in each panel indicates the voltage protocol used to evoke simulated $I_{Na(NI)}$, $I_{Na(W)}$ and $I_{Na(P)}$.

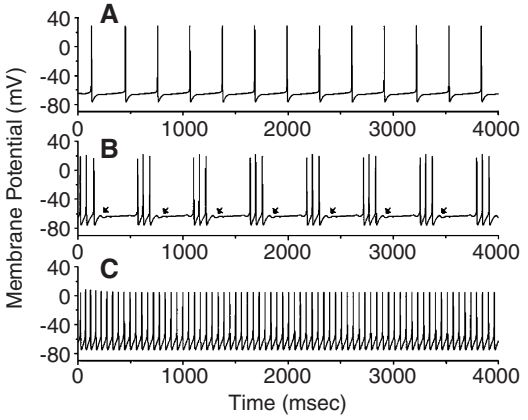

Fig. 6. Simulation modeling used to mimic the stimulatory actions of *t*-BHP on AP firing in NG108-15 neuronal cells. The detailed model equations were described in Materials and Methods. The default values for numerical parameters were shown in Table 1. The value of *f* shown in (A), (B) and (C) is 0.15, 0.4, and 0.5, respectively. When the fraction of non-inactivating Na_V channels (*i.e.*, *f*) was arbitrarily increased from 0.15 to 0.4 to mimic the action of 0.3 mM *t*-BHP, there was the increased firing of simulated APs accompanied by clustering activity and sub-threshold membrane oscillations (indicated by arrows) (B). When the *f* value was elevated to 0.5, the repetitive firing of APs was greatly increased with the disappearance of AP bursting (C).

or neuroendocrince cells *in vivo*.

Discussion

The major findings of this study were that in differentiated NG108-15 neuronal cells, *t*-BHP diminished the peak amplitude of rapidly activating I_{Na} and the inactivation rate of this current; however, it did not alter the activation time course of the current. Secondly, the $I_{Na(NI)}$ elicited by a long-lasting ramp pulse was subject to an increase by *t*-BHP. Then, the I_{Na} in response to AP waveforms was reduced and the inactivation/deactivation rate of I_{Na} was slowed, when the cells were challenged with *t*-BHP. *t*-BHP could also induce sub-threshold membrane oscillations accompanied by increased firing of APs. Finally, the simulation model presented herein was used to predict that the increased fraction (*i.e.*, *f* value) of the non-inactivating Na_V channels, which mimics the *t*-BHP action, can alter the firing pattern of APs in modeled neuron. Taken together, these findings reveal that the increased amplitude of $I_{Na(NI)}$ during the exposure to oxidative stress is one of the potential mechanisms underlying the rate and pattern of repetitive firing of neuronal APs occurring *in vivo*.

In this study, the effects of the oxidizing agents (*e.g.*, *t*-BHP and AAPH) on I_{Na} in NG108-15 neuronal cells clearly are not limited to their inhibition of the peak amplitude of this current (29). A minimal effect on the *I-V* relationship of the peak I_{Na} was observed in the presence of *t*-BHP. However, an important feature of I_{Na} block caused by these oxidizing agents is that the time course of I_{Na} inactivation became slower, while no discernible change in the initial rising phase of the current was detected. In other words, blocking of I_{Na} by these agents is not instantaneous, but develops with time after the channel becomes opened, thereby producing a slowing of current inactivation. It is also clear that the effect of reactive oxygen species on the non-inactivating fraction of I_{Na} is potentially important. This notion is supported by changes in time dependence of I_{Na} during the challenge with reactive oxygen species. The inactivation time constant of I_{Na} is increased significantly, while its activation time constant remains unchanged. The linkage of the oxidative stress and the Na_V channel function will have significant implications on the gating of these channels (14, 29).

In this study, with the aid of a combination of experimental observations and computer modeling, the $I_{Na(NI)}$ present in differentiated NG108-15 neuronal cells was increased following oxidative stress, while the $I_{Na(W)}$ was reduced. Cell exposure to riluzole or oxcarbazepine was able to reverse the *t*-BHP-induced increase of $I_{Na(NI)}$. Our work also provides new evidence for a significant contribution of $I_{Na(NI)}$ to the sub-threshold membrane oscillations associated with a clustering-like activity. It is possible that a certain fraction of this current is derived from oxidation of Na_V channels *via* reactive oxygen metabolites under certain pathological conditions (14). As a result, $I_{Na(NI)}$ could play a significant role in the firing pattern of neuronal APs. Therefore, drugs that block these channels and reduce the fraction of persistent Na_V channels (*e.g.*, riluzole or oxcarbazepine) may have, to some extent, therapeutic efficacy, assuming that their concentrations are far below those that impair nerve impulse propagation or cardiovascular function (1, 15, 30).

Many types of ion channels have been reported to respond to oxidizing agents; however, in contrast to the non-inactivating Na_V channels, their activity tends to be diminished rather than enhanced (5, 16, 27, 29). The C-terminal end of the Na^+ channels is known to contain several cysteines. These cysteine residues, along with potential disulfide bonds, are possible candidates for redox modulation. Because oxidative stress readily affects the integrity of cell membrane and the redox reagents (*e.g.*, *t*-BHP and AAPH) usually react with essential cysteine groups on Na_V channels, the activation of $I_{Na(NI)}$ by the challenge with these reagents is likely to be related to increase in the level of intracellular oxidized glutathione (16, 28). The challenge of cells (*e.g.*, NG108-15 neuronal cells) with oxidizing agents can potentially cause the formation or disruption of intermolecular mixed disulfides, resulting in conformational changes in the channel protein, eventually affecting the channel gating. The modulation of thiol groups caused by oxidative stress may well constitute a physiologically relevant control mechanism of Na_V channel function in neurons or neuroendocrine cells (25, 29). To what extent the oxidizing agents can alter the slow movement of the S4 segments in domains III and IV in Na_V channels as described previously (26, 30) also remains to be delineated.

In this study, we clearly demonstrated that both I_{Na} and $I_{Na(NI)}$ present in differentiated NG108-15 neuronal cells were modified by chemical injuries associated with oxidative stress. Oxidative stress with *t*-BHP was also able to alter the firing pattern of APs in these cells. In addition to *t*-BHP, a number of pathogenic factors have been identified to enhance $I_{Na(NI)}$ and have the potential to induce sub-threshold membrane oscillations (1, 11, 17, 29, 31). Because $I_{Na(NI)}$ can be activated at relatively negative membrane potentials (33), this current may play a significant role in the development of clustering activity following oxidative stress.

Neuronal bursting is a type of discharge observed in different kinds of neurons during many stereotypic pattern-generated behaviors, such as locomotion, respiration, and mastication (2, 6). The bursting mechanism also involves the integration of ligand-gated synaptic activity and intrinsic membrane properties (7, 8, 31, 35). Modification of bursting activity by oxidizing agents could have an important impact on repetitive motor pattern essential for physiological function. Alternatively, in dorsal root ganglion neurons, the enhanced ectopic discharge occurring during nerve injury is associated with chronic pain and sub-threshold oscillations (1). It remains to be determined to what extent any oral-motor disorders resulting in abnormal jaw movements and pain states are linked to dysfunction of I_{Na} and/or $I_{Na(NI)}$ accompanied by sub-threshold membrane oscillations in brainstem neurons.

With the aid of a theoretical model presented in this study, we clearly showed that the oxidizing agents increased the fraction (*i.e.*, *f* value) of non-inactivating Na_V channels and effectively enhanced the firing of APs accompanied by a clustering activity and sub-threshold membrane oscillations. The simulation results prompted us to propose that the activity of persistent Na^+ channels may contribute to the firing behavior of NG108-15 neuronal cells. It should be mentioned, in this context, that our simulation in-

corporates some simplifying assumptions and may not be extrapolated to other types of neurons. However, the quantitative model presented herein is able to complement the experimental observations by providing insight into persistent Na_V channels, which can impinge upon the electrical behavior of neurons or neuroendocrine cells *in vivo*. Our simulation results also support the notion that changes in the fraction of the non-inactivating Na_V channels caused by oxidizing agents may affect the functional activity of neurons *in vivo*. Taken together, in addition to the inhibition of rapidly activating I_{Na}, our results strongly suggest that the actions caused by oxidizing agents could be associated with the direct activation of $I_{Na(P)}$ present in neurons.

Acknowledgments

This research project was funded by the National Science Council (NSC-98-2320-B-006-027-MY3), Taiwan. This work was also supported in part by a grant from Buddhist Dalin Tzu-Chi General Hospital (DTCRD98-08). Many thanks are due to Hsuan Peng and Yung-Han Wu for their technical assistance. The authors are also grateful to Paul Steed for improving the language.

Statement of Interest

None of the authors in this study have any potential conflict of interest nor financial interests to disclose.

References

1. Amir, R., Argoff, C.E., Bennett, G.J., Cummins, T.R., Durieux, M.E., Gerner, P., Gold, M.S., Porreca, F. and Strichartz, G.R. The role of sodium channels in chronic inflammatory and neuropathic pain. *J. Pain* 7: S1-S29, 2006.
2. Bradley, N.S. and Smith, J.L. Neuromuscular patterns of stereotypic hindlimb behaviors in the first two postnatal months. I. stepping in normal kittens. *Brain Res*. 466: 37-52, 1988.
3. Cannon, S.C., Brown, R.H.Jr. and Corey, D.P. Theoretical reconstruction of myotonia and paralysis caused by incomplete inactivation of sodium channels. *Biophys. J*. 65: 270-288, 1993.
4. Chen, B.S., Peng, H. and Wu, S.N. Dexmedetomidine, an α_2-adrenergic agonist, inhibits neuronal delayed-rectifier potassium current and sodium current. *Br. J. Anaesth*. 103: 244-254, 2009.
5. Ciorba, M.A., Heinemann, S.H., Weissbach, H., Brot, N. and Hoshi, T. Modulation of potassium channel function by methionine oxidation and reduction. *Proc. Natl. Acad. Sci. U.S.A.* 94: 9932-9937, 1997.
6. Conway, B.A., Reid, C. and Halliday, D.M. Low frequency corticomuscular coherence during voluntary rapid movements of the wrist joint. *Brain Topogr*. 16: 221-224, 2004.
7. Cooper, D.C. The significance of action potential bursting in the brain reward circuit. *Neurochem. Int.* 41: 333-340, 2002.
8. D'Ascenzo, M., Podda, M.V., Fellin, T., Azzena, G.B., Haydon, P. and Grassi, C. Activation of mGluR5 induces spike after depolarization and enhanced excitability in medium spiny neurons of the nucleus accumbens by modulating persistent Na^+ currents. *J. Physiol*. 587: 3233-3250, 2009.
9. Ermentrout, G.B. Stimulating, Analyzing, and Animating Dynamical System: A Guide XPPAUT for Researchers and Students. Philadelphia, PA, USA: Society for Industrial and Applied Mathematics (SIAM), 2002.
10. Fekete, A., Franklin, L., Ikemoto, T., Rózsa, B., Lendvai, B., Sylvester Vizi, E. and Zelles, T. Mechanism of the persistent sodium current activator veratridine-evoked Ca elevation: implication for epilepsy. *J. Neurochem*. 111: 845-756, 2009.
11. Fransén, E., Alonso, A.A., Dickson, C., Magistretti, J. and Hasselmo, M.E. Ionic mechanisms in the generation of subthreshold oscillations and action potential clustering in entorhinal layer II stellate neurons. *Hippocampus* 14: 368-384, 2004.
12. Gage, P.W., Lamb, G.D. and Wakefield, B.T. Transient and persistent sodium currents in normal and denervated mammalian skeletal muscle. *J. Physiol*. 418: 427-439, 1989.
13. Hall, E.D. and Bosken, J.M. Measurement of oxygen radicals and lipid peroxidation in neural tissues. *Curr. Protoc. Neurosci. Chapter* 7: Unit 7.17.1-51, 2009.
14. Hammarström, A.K.M. and Gage, P.W. Hypoxia and persistent sodium current. *Eur. Biophys. J*. 31: 323-330, 2002.
15. Huang, C.W., Huang, C.C., Lin, M.W. and Wu, S.N. The synergistic inhibitory actions of oxcarbazepine on voltage-gated sodium and potassium currents in differentiated NG108-15 neuronal cells and model neurons. *Int. J. Neuropsychopharmacol*. 11: 597-610, 2008.
16. Huang, M.H., Wu, S.N. and Shen, A.Y. Stimulatory actions of thymol, a natural product, on Ca^{2+}-activated K^+ currents in pituitary GH_3 cells. *Planta Medica* 71: 1093-1098, 2005.
17. Janahmadi, M., Goudarzi, I., Kaffashian, M.R., Behzadi, G., Fathollahi, Y. and Hajizadeh, S. Co-treatment with riluzole, a neuroprotective drug, ameliorates the 3-acetylpyridine-induced neurotoxicity in cerebellar Purkinje neurons of rats: behavioural and electrophysiological evidence. *Neurotoxicology* 30: 393-402, 2009.
18. Kawaguchi, A., Asano, H., Matsushima, K., Wada, T., Yoshida, S. and Ichida, S. Enhancement of sodium current in NG108-15 cells during neuronal differentiation is mainly due to an increase in NaV1.7 expression. *Neurochem. Res*. 32: 1469-1475, 2007.
19. Lin, M.W., Wang, Y.J., Liu, S.I., Lin, A.A., Lo, Y.C. and Wu, S.N. Characterization of aconitine-induced block of delayed rectifier K^+ current in differentiated NG108-15 neuronal cells. *Neuropharmacology* 54: 912-923, 2008.
20. Lo, Y.K., Wu, S.N., Lee, C.T., Li, H.F. and Chiang, H.T. Characterization of action potential waveform-evoked L-type calcium currents in pituitary GH_3 cells. *Pflügers Arch.* 442: 547-557, 2001.
21. Mittmann, T., Linton, S.M., Schwindt, P. and Crill, W. Evidence for persistent Na^+ current in apical dendrites of rat neocortical neurons from imaging of Na^+-sensitive dye. *J. Neurophysiol*. 78: 1188-1192, 1997.
22. Molnar, P. and Hickman, J.J. Modeling of action potential generation in NG108-15 cells. *Methods Mol. Biol*. 403: 175-184, 2007.
23. Peers, C., Lang, B., Newsom-Davis, J. and Wray, D.W. Selective action of myasthenic syndrome antibodies on calcium channels in a rodent neuroblastoma × glioma cell line. *J. Physiol*. 421: 293-308, 1990.
24. Rich, M.M. and Pinter, M.J. Crucial role of sodium channel fast inactivation in muscle fibre inexcitability in a rat model of critical illness myopathy. *J. Physiol*. 547: 555-566, 2003.
25. Roberts, R.A., Laskin, D.L., Smith, C.V., Robertson, F.M., Allen, E.M., Doorn, J.A. and Slikker, W. Nitrative and oxidative stress in toxicology and disease. *Toxicol. Sci*. 112: 4-16, 2009.
26. Sheets, M.F. and Hanck, D.A. Outward stabilization of the S4 segments in domains III and IV enhances lidocaine block of sodium channels. *J. Physiol*. 582: 317-334, 2007.
27. Sheu, S.J. and Wu, S.N. Mechanism of inhibitory actions of oxidizing agents on calcium-activated potassium current in

cultured pigment epithelial cells of the human retina. *Invest. Ophthalmol. Vis. Sci.* 44: 1237-1244, 2003.

28. Tanaka, K., Fujita, N., Yoshioka, M. and Ogawa, N. Immunosuppressive and non-immunosuppressive immunophilin ligands improve H_2O_2-induced cell damage by increasing glutathione levels in NG108-15 cells. *Brain Res*. 889: 225-228, 2001.
29. Wang, G.K. and Wang, S.Y. Modification of human cardiac sodium channel gating by UVA light. *J. Membr. Biol*. 189: 153-165, 2002.
30. Waxman, S.G. Channel, neuronal and clinical function in sodium channelopathies: from genotype to phenotype. *Nat. Neurosci*. 10: 405-409, 2007.
31. Wu, N., Enomoto, A., Tanaka, S., Hsiao, C.F., Nykamp, D.Q., Izhikevich, E. and Chandler, S.H. Persistent sodium currents in mesencephalic V neurons participate in burst generation and control of membrane excitability. *J. Neurophysiol*. 93: 2710-2722, 2005.
32. Wu, S.N. Simulations of the cardiac action potential based on the Hodgkin-Huxley kinetics with the use of Microsoft Excel spreadsheet. *Chinese J. Physiol*. 47: 15-22, 2004.
33. Wu, S.N., Chen, B.S., Hsu, T.I., Peng, H., Wu, Y.H. and Lo, Y.C. Analytical studies of rapidly inactivating and noninactivating sodium currents in differentiated NG108-15 neuronal cells. *J. Theor. Biol*. 259: 828-836, 2009.
34. Wu, S.N., Chen, B.S., Lin, M.W. and Liu, Y.C. Contribution of slowly inactivating potassium current to delayed firing of action potentials in NG108-15 neuronal cells: experimental and theoretical studies. *J. Theor. Biol*. 252: 711-721, 2008.
35. Yue, C.Y., Remy, S., Su, H.L., Seck, H. and Yaari, Y. Proximal persistent Na^+ channels drive spike after depolarizations and associated bursting in adult CA1 pyramidal cells. *J. Neurosci.* 25: 9705-9720, 2005.